Numerical modelling of the Laminaria concept with coupled mooring and PTO system

Rémy CR Pascal[♣1], Benjamin Gendron[★2], Adrien Combourieu[★3]
[♣]*INNOSEA Ltd*
ETTC, Alrick Building,Max Born Crescent, Edinburgh - UK
[1]remy.pascal@innosea.fr
[★]*INNOSEA*
1 rue de la No, 44321 Nantes Cedex 03, France
[2]benjamin.gendron@innosea.fr
[3]adrien.combourieu@innosea.fr

***Abstract*—Within the LAMWEC project, INNOSEA has been responsible for the tank test of the Laminaria WEC. This WEC concept solves the compromise between security and performance by introducing a dual load management system. The average loads are controlled by gradually lowering the device in the water column for increasing H_S. In addition, a PTO overdrive limits extreme loads. The dual load management system allows nearly constant loads and power production irrespective of H_S.**
The objectives of the $1:16^{th}$ scale tests in the COAST lab were to prove the dual load management system and to characterize the mooring loads in representative sea conditions. Laminaria provided the model. INNOSEA designed the test plan, analysed the data and produced the final report.
The loads' histograms show that the PTO overdrive concept can effectively limit extreme loads. Indeed, the histograms of the tests which activated the PTO overdrive are distorted compared to the typical expectations, showing a limited tail and a bulge of occurrences close to the PTO overdrive threshold. The analysis of the statistical distributions parameters fitted to the mooring load histograms shows that gradually submerging the device is an effective way to manage the average loads.

***Index Terms*—WEC, tank tests, load management, submergence, mooring loads**

I. Introduction

The development of wave energy in the past decades has been deeply guided by the need to design devices with a strong compromise at the heart of the concepts: creating devices that maximizes the energy to recover from the waves, hence maximising the wave forces on the bodies for the usual wave periods while at the same time designing for survivability for similar wave periods [1] [2]. This is a compromise unique to wave energy converters (WECs) within the world of offshore structure, as other structures are normally designed to reduce wave loads at the usual wave periods.
In addition to this defining compromise, the oscillatory nature of the waves and the seasonal variability of the resource imposes challenges in the design of efficient Power take Off (PTOs) for WECs [3] [4]. Especially for PTOs which are not including a stage of energy storage before the primary generators, dimensioning a PTO that is both efficient at the low average load levels encountered in production sea states, and large enough to accommodate for the large variation of powers, is an issue not faced by other types of renewable energy converters.
The Laminaria concept answers both challenges by introducing a system to manage the design loads of the WECs and control the PTO loads as a function of the sea states characteristics. Within the LAMWEC project, INNOSEA oversaw the tank tests and data post-processing, and the numerical modelling of the device. This study describes the numerical model work. As the utilised sea states and the post-processing are common with the experimental work, readers are encouraged to refer to [5] for the details of these aspects.

II. The Laminaria Concept

A. General description

The Laminaria device is a small, taut moored, surge, sway, pitch and roll operated point absorber. A single vertical body interacts with the incident wave field and is free to move in the four degrees of freedom mentioned above. The motions are linked to the generators through the mooring ropes (active mooring device). The device is able to convert wave power from all wave directions. In normal operation, the system sits in the water with the top of the device near the surface, as shown in Fig. 1. The four symmetric mooring lines are connected to a central rope connection point. From there, each mooring line runs to a pulley fixed to the seabed. The mooring line then runs to a pulley connected to the device, and finally connects to its respective drum on one of the two main shafts and finally drives the generator. The lines are paired by being linked to a single drum two by two. The combined length of each pair of mooring lines is constant for a given device submergence: as one side of the line is shortened by being rolled into the drum, the other side of the line is extended by the same length by rolling out of the drum. Lines 2 and 3 are at the front, facing the incoming waves, and lines 1 and 4 are at the back.

B. PTO law and load management

When the wave-induced mooring loads exceed a predefined threshold, the main body of the Laminaria concept is lowered into the water column, down to the point where the mooring

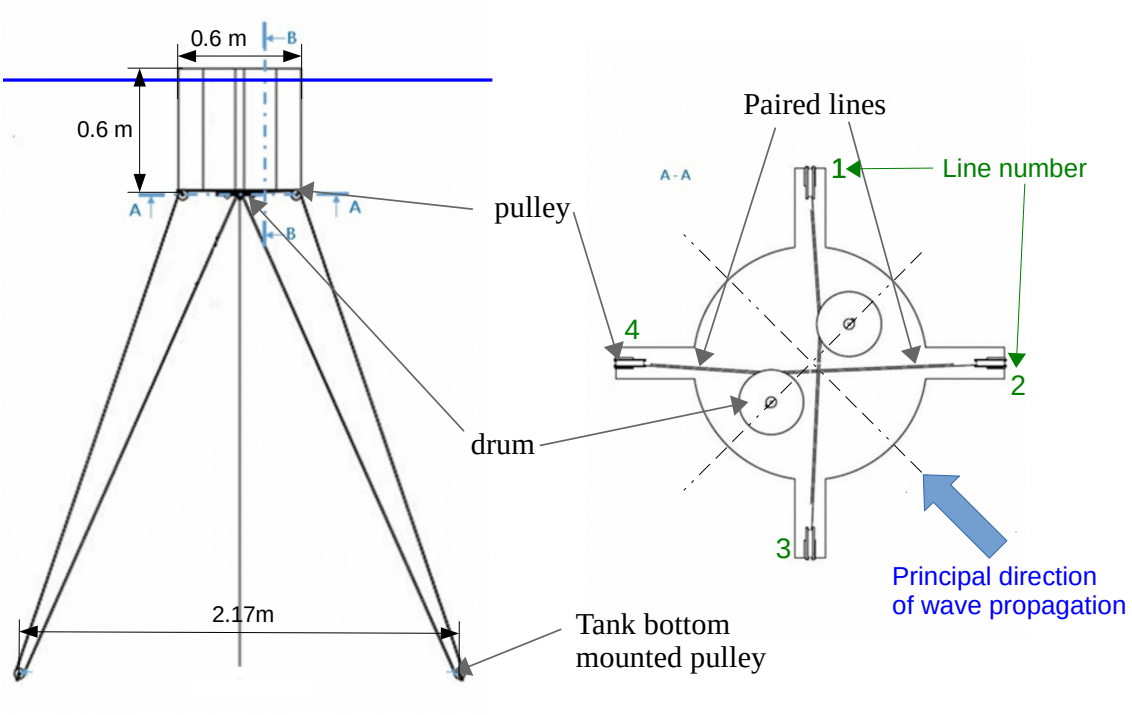

Fig. 1. Schematic view of the Laminaria WEC. Line numbers with respect to the main wave direction of propagation are indicated.

loads are close to the maximum allowed loads in nominal conditions. This ensures nominal power production even during the heaviest of storms without undergoing excessive forces. The mechanism used to lower the device is integrated to the primary mooring systems (similar concepts have been explored in other WECs [6], [7]). The mooring lines are simply spooled on their drums to reduce their overall length.

An additional system is built in the PTO control law. The PTO is regulated so that the mooring line drum velocity is proportional to the torque difference applied on the drums by the opposite mooring lines. However, if the instantaneous torque exceeds a predefined threshold (the overdrive limit), the PTO law is set to let the drum speed accelerate quickly in order to limit the torque, thus limiting the load imbalance in the mooring lines. The effective PTO control law can, therefore, be described as piecewise linear as shown schematically in Fig. 2. Together, the submergence should control the average load levels in the lines and the overdrive mechanism should limit the extrema. *To the best knowledge of the authors, the combination into the same concept of a method to control the average loads and curtail extrema without stopping production and without additional mechanisms is unique to the Laminaria concept.*

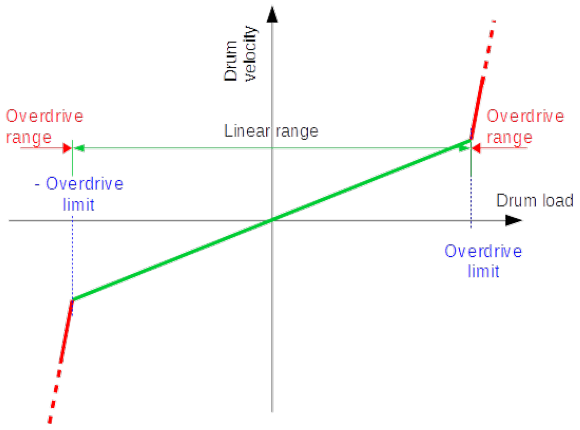

Fig. 2. Schematic of the PTO control law.

III. Tank tests and model configurations

The model was tested within the LAMWEC project in the Plymouth tank in 2016 at an indicative scale factor of $1 : 19.67^{th}$. Details of the tanks tests and the model used are available in [5]. The tests results are used to evaluate and validate the numerical models.

During these tests, several mooring configurations were employed in irregular waves. There was no prior guidance to which submergence should be achieved for a given sea states conditions. This led to consider three levels of submergence additionally to the nominal position: 30cm, 40cm and 50cm at tank scale.

The submergence levels were obtained by shortening the mooring lines for the 50cm configurations, and then use the movable floor to reach the other conditions. This limited the installation time between configurations. The induced change of water depth is below 6.7% in all cases and effect of the sea state is neglected. The mooring configurations are shown in Fig. 3.

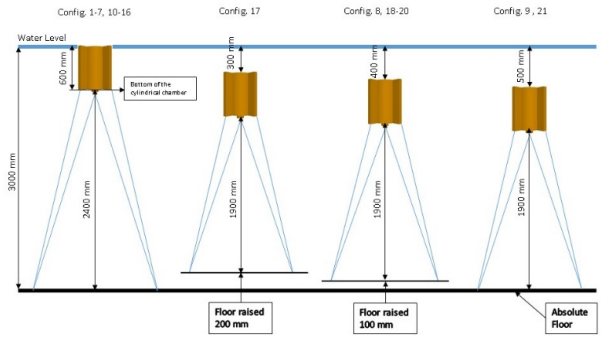

Fig. 3. Mooring configurations

For loads estimation, the results corresponding to configurations 6 (nominal submergence), 8 (40 cm submergence), and 9 (50 cm submergence) are used. The other configurations numbers correspond to different PTO settings that were explored for performance optimisation.

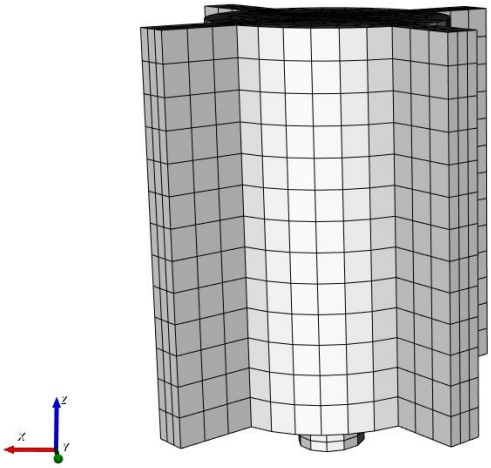

Fig. 4. mesh with 1315 faces

IV. Numerical model

A. The InWave framework

InWave, developed by INNOSEA, is a complete WEC modelling tool based on linear potential theory coupled with a time-domain multi-body dynamic solver. The potential flow theory is based on the Boundary Element Method (BEM) with constant panels, a method commonly used for sea-keeping and wave-structure interactions. It can compute the pressure variation and free surface perturbations without having to mesh the entire fluid domain, and with the use of Green functions to represent the free-surface, only the floating bodies have to be meshed. Different models can be chosen in InWave for the simulation of a WEC :

- a fully linear version where the device is simulated with linear hydrodynamic matrices (added mass, hydrodynamic damping and hydrostatic stiffness matrices)
- a partially non-linear version which computes the instant immersed surface of the floating device and the resulting buoyancy force depending on the incident wave field. The radiation effects are computed with the added mass and hydrodynamic damping.

Additional features like power take-off, quadratic damping, mooring models and post-processing algorithms are also present. InWave has been validated through a code-to-code and experimental validation [8]–[10]. Its modular approach makes it possible to extend its possibilities by adding complex non-linear forces like the PTO and mooring system of the Laminaria concept.

B. Meshing and hydrodynamic database

A mesh of the tank model was produced, using the tank model dimension and a Froude scaling factor of $1:19.67^{th}$. A view of the mesh with 1315 faces is presented in Fig. 4. A mesh convergence study was performed, using 6 different mesh densities ranging from 636 to 2015 faces. The wave direction was set at 0°only, 50m water depth, and the device just protruding above the water level. The convergence was determined by visual observations of the hydrodynamic parameters results. The mesh with 1315 faces appears to be sufficient and is used for all the results presented in this study.

C. The linear model

For an efficient solution, a linear model fitting within the standard InWave model is defined. Such model requests a linearisation of the coupled mooring and PTO system, which could be represented by a set of stiffness, $\mathbf{K}$, and damping $\mathbf{D}$ matrices.

In this first approach, a 2D model is considered. The geometric constraint imposed on the device motion by the mooring line length is approximated by limiting the device motion to surge and pitch only.

The PTO/mooring system is then linearised by considering the effect of small motions and speeds around the equilibrium position of the device.

1) Surge stiffness: The stiffness coefficients k_{11} and k_{51} related to surge displacement are estimated by considering the overall mooring forces in a static displacement, as in Fig. 5. The vertical component of the force is considered constant, leading to the following expression for the matrix coefficients expressed in G, the centre of gravity:

$$k_{11} = \frac{B - W}{L} \tag{1}$$

$$k_{51} = -\frac{B - W}{L} \cdot h \tag{2}$$

2) Pitch stiffness: A small rotation θ around the centre of gravity G is considered. The combined mooring forces is applied at the point A, which coincide with A_0 for $\theta = 0$.The overall parametrisation is presented in Fig. 6. The angles are considered small ($\cos(x) = 1$, $\sin(x) = \tan(x) = 0$). This

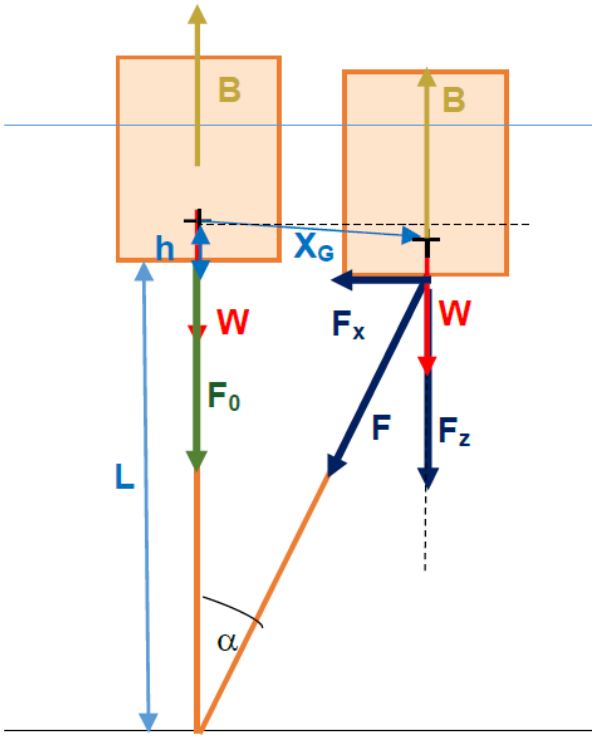

Fig. 5. Mooring with small static displacement in surge.

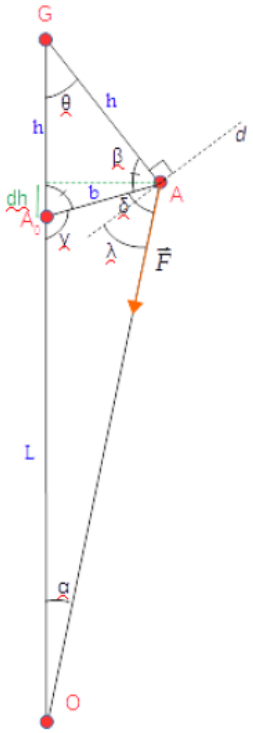

Fig. 6. Parametrisation for the estimation of the pitch related stiffness coefficients.

also allows the hypothesis that the mooring force direction is along $\overrightarrow{AO}$. The resolution leads to the stiffness coefficients k_{15} and k_{55} at point G:

$$k_{15} = -\frac{B-W}{L} \cdot h \tag{3}$$

$$k_{55} = h \cdot (B-W) \cdot \frac{h+L}{L} \tag{4}$$

3) Damping coefficients: The evaluation of the relevant coefficients of the damping matrix $(d_{11}, d_{15}, d_{51}, d_{55})$ is made by:

- assuming that the device is the equilibrium position,
- first, estimates d_{11} and d_{51} assuming only a small velocity in surge,
- second, estimates d_{15} and d_{55} assuming only a small velocity in pitch around the point O (Fig. 7). With the other coefficients equal to 0 (surge and pitch model only), the damping matrix $\mathbf{D_{G,O}}$ at point G with a speed vector at point O is complete,
- transferring the obtained damping matrix $\mathbf{D_{O,G}}$ using speed at the point O to the damping matrix $\mathbf{D_{G,G}}$ with the speed vector at the centre of Gravity G of the device.

The parametrisation considered in this section is shown in Fig. 7. As the device is considered at equilibrium, $\alpha_1 = \alpha_2 = \alpha$ and $\sigma_1 = \sigma_2 = \sigma$ in the rest of this section. The sum of the 6 forces and their moments is written at the point G. Using Eq. 6, the resultant surge force $\overrightarrow{F_{x,res}}$ and pitch moment $\overrightarrow{M_{y,CoG,res}}$ can be written as in Eq. 7 and Eq. 8:

$$\omega = qr(T_1 - T_2) \tag{5}$$

$$\Rightarrow T_1 - T_2 = \frac{d\tau}{qr^2 dt} \tag{6}$$

$$\overrightarrow{F_{x,res}} = \frac{\omega}{qr}\left[\cos\alpha - \cos\sigma\right]\overrightarrow{x} \tag{7}$$

$$\overrightarrow{M_{y,CoG,res}} = \frac{\omega}{qr}\left[h(\cos\sigma - \cos\alpha) - \frac{l}{2}\sin\alpha\right]\overrightarrow{y} \tag{8}$$

with ω the PTO drum speed, q the PTO constant, r the drum radius (assumed constant for simplicity) and $\frac{d\tau}{dt} = r \cdot \omega$ the change in mooring line length.

The objective is to link the small velocities of pitch and surge to $\frac{d\tau}{dt}$. This is done through linearisation of the trigonometric functions, and the hypothesis that the mooring lines are close to the vertical (this is true when the device is at the surface, but less as submergence increases). While the full demonstration is outside the scope of this article, the obtained values for the $D_{O,G}$ matrix are:

$$\begin{cases} d_{11} = \dfrac{1}{qr^2}\left[\cos\alpha - \cos\sigma\right]^2 \\ d_{15} = \dfrac{-l}{2qr^2}\left[\cos\alpha - \cos\sigma\right] \\ d_{51} = -\dfrac{\cos\sigma - \cos\alpha}{qr^2}\left[h(\cos\sigma - \cos\alpha) + \dfrac{l}{2}\sin\alpha\right] \\ d_{55} = \dfrac{1}{2qr^2}\left[h(\cos\alpha - \cos\sigma) + \dfrac{l}{2}\sin\alpha\right] \end{cases} \tag{9}$$

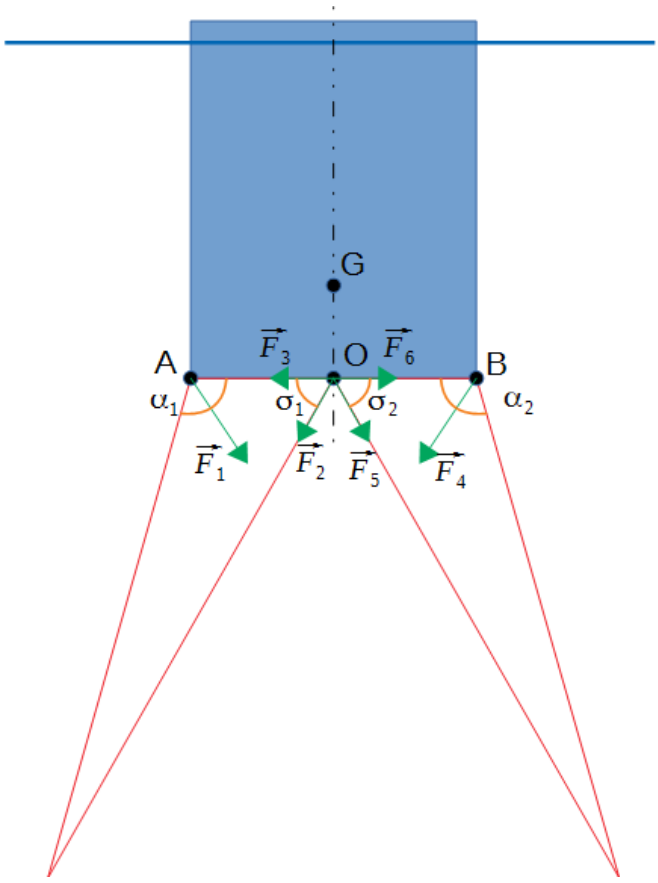

Fig. 7. Parametrisation for the estimation of the pitch related stiffness coefficients.

The damping matrix is now obtained considering a speed vector $\overrightarrow{V_{O,1/0}}$ between the device (1) and the absolute coordinate system (0) at the point O. However, the InWave framework request the damping matrix to consider the motion of the CoG. The following relation follows:

$$\begin{bmatrix} \overrightarrow{F_{G,1/0}} \\ \overrightarrow{M_{G,1/0}} \end{bmatrix} = -\mathbf{D_{O,G}} \begin{bmatrix} \overrightarrow{V_{O,1/0}} \\ \overrightarrow{\Omega_{1/0}} \end{bmatrix} = -\mathbf{D_{G,G}} \begin{bmatrix} \overrightarrow{V_{G,1/0}} \\ \overrightarrow{\Omega_{1/0}} \end{bmatrix} \quad (10)$$

with the left term the effort wrench at point G between the device and the reference, and $\Omega_{1/0}$ the rotation vector between the device and the reference.
Assuming small motions ($\overrightarrow{GO} \cdot \overrightarrow{x} \simeq 0$), Eq. 11 is obtained:

$$\begin{bmatrix} \overrightarrow{V_{O,1/0}} \\ \overrightarrow{\Omega_{1/0}} \end{bmatrix} = \begin{bmatrix} \mathbf{I_3} & \mathbf{S}(\overrightarrow{GO}) \\ \mathbf{0_3} & \mathbf{I_3} \end{bmatrix} \cdot \begin{bmatrix} \overrightarrow{V_{G,1/0}} \\ \overrightarrow{\Omega_{1/0}} \end{bmatrix} \quad (11)$$

$$\text{with} \quad \mathbf{S}(\overrightarrow{GO}) = \begin{bmatrix} 0 & -h & 0 \\ h & 0 & 0 \\ 0 & 0 & 0 \end{bmatrix} \quad (12)$$

Using Eq. 11 into Eq. 10, the expression of the $D_{G,G}$ matrix is obtained as:

$$\mathbf{D_{G,G}} = \mathbf{D_{O,G}} \cdot \begin{bmatrix} \mathbf{I_3} & \mathbf{S}(\overrightarrow{GO}) \\ \mathbf{0_3} & \mathbf{I_3} \end{bmatrix} \quad (13)$$

The complete linear InWave model can then be specified using the stiffness and damping matrices. No specific PTO should be added to the model. The instantaneous power P absorbed by the device is obtained as $P = D_{G,G} \cdot \overrightarrow{V_{G,1/0}}$ during post processing of the simulations.

4) limitation of linear model: The mooring/PTO model is designed to integrate within the standard InWave framework, and therefore benefits for the advantages of it, such as speed of execution and the possibility to includes some non-linear hydrodynamics. The overall model, however, relies on potential flow theory, and therefore viscous effects are neglected.
The linearisation of the mooring/PTO problems also imposes restrictions on the PTO law which can be implemented. Only linear PTOs can be considered, and therefore the overdrive mechanism (see Section II-B) cannot be implemented. This limits the scope of the linear model.
Additionally, the formulation of the model only allows to obtain the load difference between the mooring lines, but not the load absolute value. A further hypothesis of symmetric loading formulation must be done to infer the absolute mooring loads.
Finally, the model resolution is limited to small motions (consistent with hydrodynamic limitations) around the equilibrium position and requires the mooring lines to be close to the vertical. This last element constraint the domain of validity of the model when considering submerged configurations.

D. Including quadratic damping

To compensate some of the limitations of the base linear model, a quadratic damping matrix was introduced into the framework. Such introduction allows limiting the amount of motion close to the device resonance, which, in the case of linear models can become unrealistic (see [11]). Such quadratic damping matrix is not directly a model for the viscous damping, but it can approximate it in a first approach. The coefficients of the quadratic matrix were calibrated using the tank data, and includes the cross coefficients between pitch and surge.

1) limitation of the linear model with quadratic damping: Introducing a quadratic damping matrix which coefficients are calibrated using tank testing data does improve the model realism, but it limits the applicability of the model. New device shape, or changes to the device configuration that significantly changes its behaviour might request different quadratic damping coefficients. This could not be confirmed before new tank tests, and therefore a model which requires calibrated coefficients cannot be used to explore the device design space beyond the close range for which the coefficients have been calibrated.

E. The non-linear model

As the linear model, even with some viscosity, exhibits significant limitations, it was necessary to consider a non-linear model of the PTO/mooring system. The framework considered is to remove the stiffness and damping matrices used in the previous model, and to use an entry point within the InWave solver to add a bespoke mooring/PTO force. The

viscosity matrix devised for the linear model is kept.
The non-linear model considered is still a 2D case, with the 6 mooring forces shown in Fig. 7. The forces are expressed in the absolute coordinate system, as a function of the line tensions T_1 and T_2, and their moments are defined at the centre of gravity G of the device. The sum of the forces and moments lead to 3 expressions, in surge, heave and pitch. To obtain a value of these forces at each time of the simulation, it is necessary to estimate the line tensions directly.
Eq. 6 is providing one equation, and a second equation on the line tensions is obtained by assuming that the static part of the heave force is dominant over the dynamic part, allowing the sum of forces along the vertical axis to be equalised to $W - B$, with W the device weight and B the buoyancy. The equations can be written in the following form:

$$\mathbf{A} \cdot X = \mathbf{B} \tag{14}$$

$$\text{with } \mathbf{B} = \begin{bmatrix} \dfrac{d\tau}{qr^2 dt} \\ W - B \end{bmatrix} \quad X = \begin{bmatrix} T_1 \\ T_2 \end{bmatrix} \quad A = \begin{bmatrix} 1 & -1 \\ a & b \end{bmatrix} \tag{15}$$

$$a = -2\cos\frac{\alpha_1}{2}\sin\left(\frac{\alpha_1}{2} + \theta\right) - \sin\sigma_1 - \sin\theta \tag{16}$$

$$b = \sin\theta - 2\cos\frac{\alpha_2}{2}\sin\left(\frac{\alpha_2}{2} + \theta\right) - \sin\sigma_2 \tag{17}$$

The angles are defined on Fig. 7. The solution can the be found as $X = \mathbf{A}^{-1} \cdot \mathbf{B}$.
One of the key advantages of the non-linear model is the possibility to implement the overdrive mechanism built into the PTO law. Implementing it requires a different PTO equation depending on the tension difference $T_1 - T_2$ between the lines. At the overdrive limit point, the drum velocity can be described by two equations:

$$\omega(\Delta T_{lim}) = qr\Delta T_{lim} = q'r\Delta T_{lim} + cst \cdot sgn(\omega)$$

with $cst = r\Delta T_{lim}(q - q')$, $\Delta T = (T_1 - T_2)$ and q' the PTO constant when using the overdrive. The relation for $(T_1 - T_2)$ when using the overdrive is derived:

$$\Rightarrow (T_1 - T_2) = \left(\frac{d\tau}{rdt} - cst \cdot sgn(\omega)\right)\frac{1}{qr} \tag{18}$$

Additionally, the non-linear model resolves directly the mooring line loads and not only the loads' imbalance as the previous models based on linearised moorings. This provides better design inputs for the moorings lines and anchoring system, and it opens the way to introduce second order wave effect into the hydrodynamics modelling.

F. Future development

Based on the 2D non-linear model, a 3D version of the model is currently under development. The model will expand the device degree of freedom to sway and roll, and will, therefore, allow the simulation of directional seas. The resolution of the four independent mooring line tensions is permitted by the two separate PTO equations, the quasi-static hypothesis on the heave degree of freedom, and the additional hypothesis on the yaw degree of freedom. From experimental observations, the yaw motion is minimal, and the mooring configuration provides a substantial yaw stiffness. This justifies the choice of blocking the yaw motion, and then to assume that the sum of torques along the yaw axis is null.

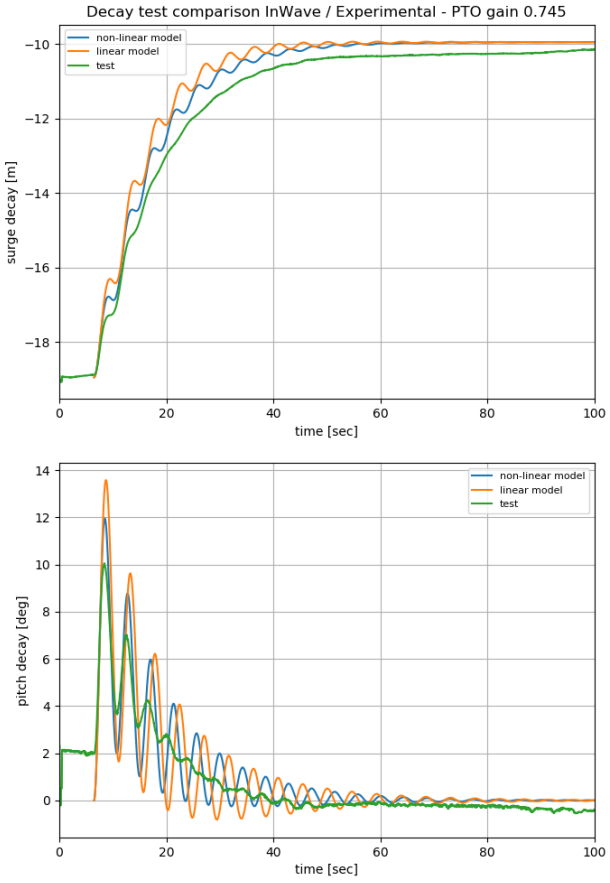

Fig. 8. Coupled pitch and surge decay tests compared to experimental data (green curve) for the linear (orange curve) and non-linear model (blue curve). In both cases, the quadratic damping is not activated.

V. RESULTS

A. Decay tests

Fig. 8 shows the decay tests of the linear and non-linear models (no quadratic damping in the models, linear PTO) compared to experimental data. Due to the model concept, the surge and pitch decay tests must be coupled, with the PTO active. The PTO constant is defined from the experimental data. Both comparisons show that the selected model formulations are adequate to represent the surge and pitch coupling observed in the experiment. However, it is clear from these plots that the simulations are underdamped, which justify the need to introduce quadratic damping. Regarding the oscillations periods, it is clear that the experimental pitch periods observed are shorter than the one predicted by the simulations, and that the non-linear model shows a significant improvement on that issue over the linear model. As the

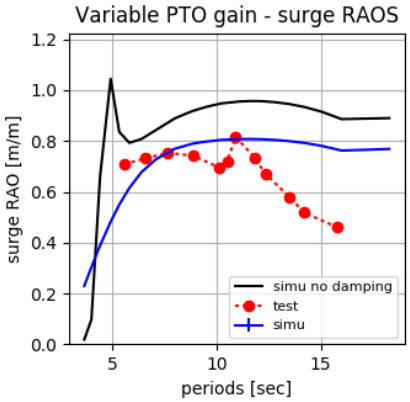

Fig. 9. Surge RAO from the linear models (in black without quadratic damping and in blue with it) compared to experimental data (red dots).

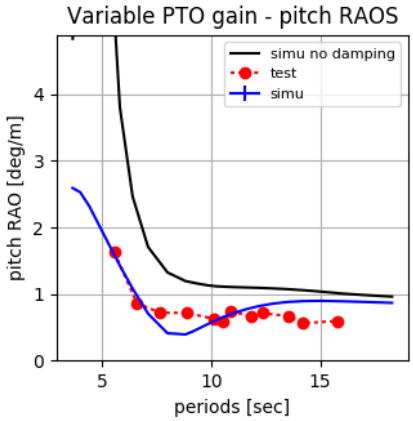

Fig. 10. Pitch RAO from the linear models compared to experimental data.

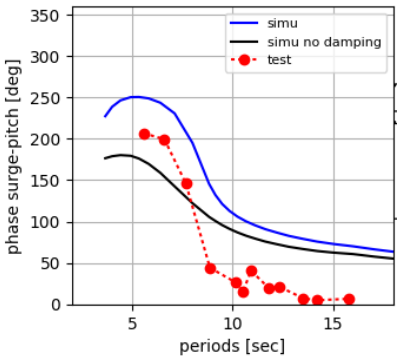

Fig. 11. Pitch and surge phase difference from the linear models compared to experimental data (red dots).

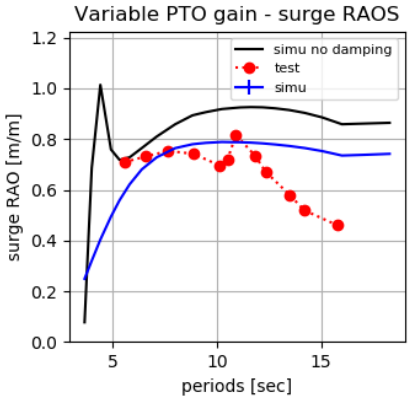

Fig. 12. Surge RAO from the nonlinear models (in black without quadratic damping and in blue with it) compared to experimental data (red dots).

decay test motions are large, it shows that the linear model formulation should only be acceptable for small motions. The difference between the experimental data and the non-linear mooring are most probably due to the hydrodynamic limitation due to the potential flow theory, and the fact that the PTO characteristics in the tests are not completely linear (see [12]).

B. Regular wave tests

As for the decay tests, regular wave simulations were conducted and compared with the experimental data. The periods considered at full scale are 3.5 to 18 seconds, with a 0.5 seconds gap. For the linear model without damping, amplitudes of 0.01m are used, and 1m for the linear model with quadratic damping. The PTO settings were obtained through linearisation of the experimental PTO characteristics, and varies with the wave period.

Fig. 9 and Fig. 10 presents the surge and pitch RAOs compared to the experimental data. The introduction of the quadratic damping matrix allows a much better match between the numerical results and the tank tests. The large peak of performance predicted in the base linear model is properly damped, and the order of magnitude of the RAOs is similar to the experimental results.

Both models exhibit significant discrepancies for the long periods, especially in surge. For these cases, the introduction of a quadratic damping matrix appears to have a limited effect. The decrease in the surge RAO at the longer periods observed in the tank tests is probably not due to viscous losses. The differences between numerical and experimental results are expected to come mainly from the difference in the PTOs and the linearisation of the mooring/PTO efforts.

In Fig. 11, the phase between the surge and pitch motions is shown as a function of the wave period. it was identified as a key performance indicator in [12]. The trend in the phase difference appears to be well represented, but significant differences between experimental data and numerical models remain, with and without quadratic damping. As for the RAOs, an important part of the observed difference is expected to be linked to the PTO characteristics of the experimental data.

Using the same regular wave inputs, the RAOs and pitch-surge phase difference from the non-linear models (with and without quadratic damping) are presented in Fig. 12 to Fig. 14. The results of the non-linear models are comparable to the linear ones, albeit some improvement (smaller gap with experimental data) at the longest periods especially in pitch and in the phase difference can be observed. This gives confidence that both

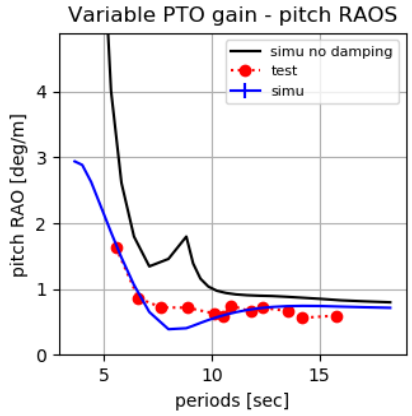

Fig. 13. Pitch RAO from the non-linear models compared to experimental data.

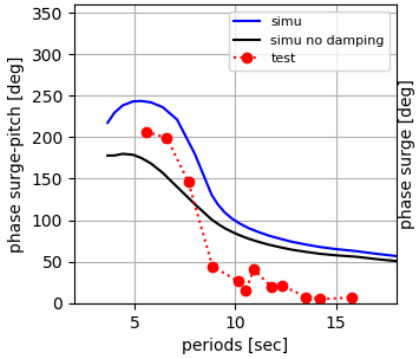

Fig. 14. Pitch and surge phase difference from the non-linear models compared to experimental data.

models are well formulated, and it highlights the benefits of the non-linear models.

The regular wave results show that the basic linear model is not sufficient in itself. This model can potentially be used to study the effect of the device design parameters over the device performance and to compare configurations relative to each other, but it should not be used to obtain quantitative values as inputs for design. On the contrary, the introduction of the quadratic damping shows that once calibrated, realistic behaviour can be obtained. Finally, the non-linear model with quadratic damping is extending the range of validity of the simulations, and further study should characterise its performances, especially using PTO characteristics closer to the experimental ones.

C. Irregular wave tests

Irregular waves were not run with the linear model without quadratic damping, as the results in regular waves were deemed to be too unrealistic. Therefore, only results with the quadratic damping activated and from the non-linear model (with quadratic damping) are available.

Following the principle topic of the LAMWEC project, the results are focused on the characterisation of the mooring line loads. The objective is to assess if the numerical model could

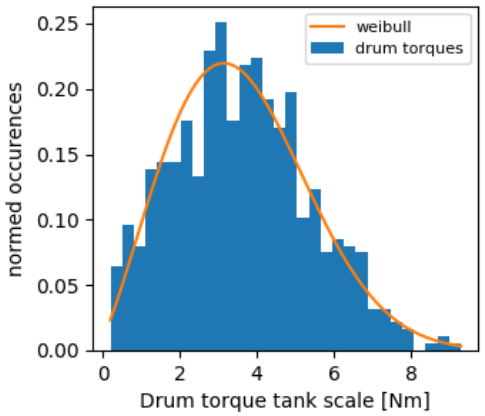

Fig. 15. Drum torque histogram from the linear model with quadratic damping, Irregular sea states 16.

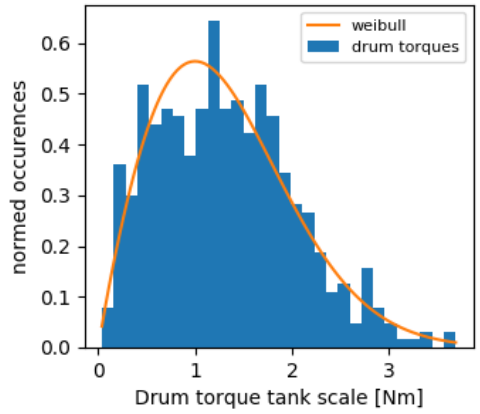

Fig. 16. Drum torque histogram from the linear model with quadratic damping, Irregular sea states 23.

provide valuable inputs for design for the anchor and mooring parts. Histogram of the PTO drum loads and line tension are obtained from the simulations results, and Weibull minimum statistical distributions are fitted to the data where possible. The characteristics of the statistical distribution can then be compared to the experimental data. The process and the sea states are described in [5].

1) Qualitative observations: Fig. 15 and Fig. 16 show the drum torque histogram and fitted statistical distribution for irregular wave 16 and 23, using the linear mooring with quadratic damping results. The histogram shape obtained are similar to the experimental data figures, and the statistical distribution utilised appears adequate.

Fig. 17 shows the same sea state as Fig. 15 modelled with the non-linear model, including quadratic damping. The histogram shape is different, with more occurrences concentrated on the histogram left. The statistical distribution again appears to provide a good fit for the data, and therefore both model could potentially be used to characterise mooring loads.

2) Comparisons of statistical distributions parameters: For the purpose of PTO dimensioning and fatigue calculation, the

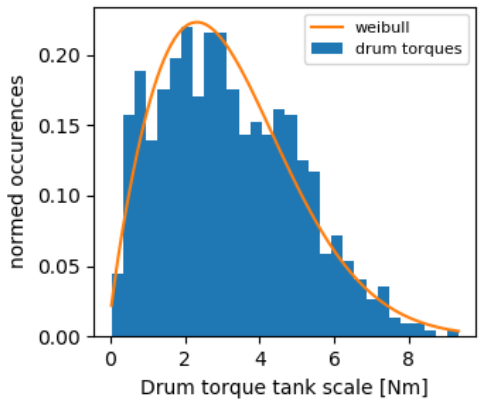

Fig. 17. Drum torque histogram from the non-linear model with quadratic damping, Irregular sea states 16.

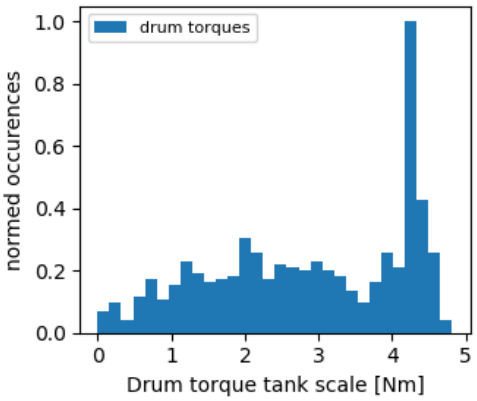

Fig. 20. Drum torque histogram from the non-linear model with quadratic damping and piecewise linear PTO, Irregular sea states 16.

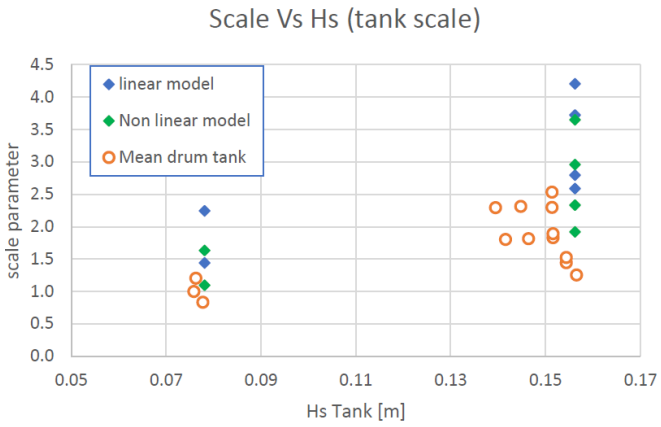

Fig. 18. Scale parameters of the distribution as a function of H_S.

values of the statistical distribution parameters fitted to the tank and the simulation results are compared and shown in Fig. 18 and Fig. 19.

The figures show that the numerical models present the same trends with regard to the main sea states parameters than the experimental data. This again gives confidence on the model formulation, and show that the models can be used

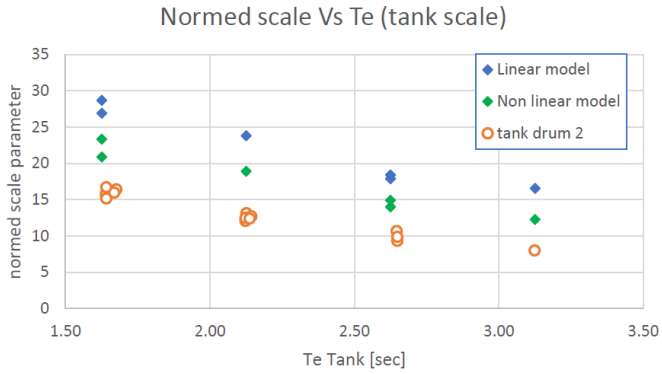

Fig. 19. Normed scale parameters of the distribution as a function of T_E.

for relative comparisons between configurations (assuming the quadratic damping characteristics are similar). However, the numerical models still overestimate the experimental results, as the *scale* parameter is showing: higher *scale* parameters indicate higher values. On this aspect, the non-linear model appears to be closer to the experimental data in all cases tested. As for the regular wave results, the differences between numerical and experimental data are expected to be due to the hydrodynamic formulation of the models based on linear potential flow theory, and the differences between the idealised PTO characteristics of the numerical models and the actual PTO characteristics obtained in the tank.

3) non linear PTO results: A major justification to introduce the non-linear model was the necessity to lift the principal limitations of the linear models, i.e. the impossibility to implement a non-linear PTO and the difficulty in modelling the submerged configurations.

Fig. 20 shows the results of the non-linear model including a non-linear PTO. The threshold for the overdrive limit (see Fig. 2) is set at $\pm 80\,N$ of load imbalance between the lines. The first part of the histogram between $0\,Nm$ and $4\,Nm$ is very similar to the one shown in Fig. 17. However, the non-linear PTO law compressed all the loads above the overdrive limit, and a large peak of occurrences can now be observed. The maximum drum loads have been reduced from $> 8\,N$ to $< 5\,N$. These results show that the numerical model is able to implement the specific control law of the Laminaria model and that it can be used to demonstrate the concept and study the influence of the parameters of such law.

4) Usability: The computation time for the model with the different options is reported. When non-linear hydrostatic forces are used, the buoyancy *B* of Eq. 15 is re-evaluated at every time step.

The cpu times, for the calculation of a 3h long irregular simulation, using the different numerical models are presented in table V-C4. The calculations were done with a single $2.5Ghz$ core for each simulation.

It can be seen that when using linear hydrodynamic forces, the non linear resolution of the mooring forces does not increase

TABLE I
CPU TIME TO OBTAIN 1H SIMULATION RESULTS ON IRREGULAR WAVES, FOR THE DIFFERENT MODELS.

hydrostatique	**Froude Krylov**	**mooring**	**PTO**	**time**
linear	linear	linear	linear	$<$ 3min
linear	linear	non linear	linear	$<$ 4min
non linear	linear	linear	linear	9h
non linear	non linear	linear	linear	15h
non linear	non linear	non linear	linear	32h
linear	linear	non linear	non linear	$<$ 4min

the computing time significantly. This model can therefore be used for all the numerical modelling activities without generating excessive computational time.

VI. Future model requirements

As the 3D formulation of the non-linear model is currently implemented, the future model requirements will be the inclusion into the hydrodynamic modelling the 2^{nd} order wave induced forces, and a model of the quadratic damping based on the device description instead of the empirical calibration of a damping matrix. This first development will permit the correct modelling of the equilibrium position with the waves, and therefore of a static imbalance of the mooring lines load. The second development, currently expected through Morrison modelling, will expand the model validity to other configuration with different drag characteristics.
The current and future models will also require to be validated with new experimental data, in which the PTO characteristics are closer to the desired PTO law control.

VII. Conclusion

Several level of numerical models have been defined within the LAMWEC project, and their results have been compared with experimental data to assess their validity. The observations shows that a first linear modelling of the combined mooring and PTO system, limited to pitch and surge only, might be sufficient to compare device configurations but cannot be used for quantitative studies and as to provide inputs for design. The model is also limited to the non submerged cases, and non-linear PTO laws cannot be implemented.
The addition of a calibrated quadratic damping matrix with pitch and surge cross term allows the linear mooring/PTO model to provides results closer to the experimental data. The domain of validity of the model cannot be completely established with the current experimental data (March 2016), but this model is expected to be valid within some limitations.
To alleviate some of the limitations linked to the formulation of the mooring and PTO system, a non-linear model was developed, still in 2D. The models relies on a quasi-static hypothesis for the heave forces. This model shows a closer agreement with the experimental data than the linear model, but requires longer computing times. As for the linear mooring model with quadratic damping, the domain of validity of the model cannot be established formally with the current experimental data. The non-linear model is however expected to form the base of a good compromise between performance and accuracy.
The features of the non-linear model, especially the possibility of the model to implement non-linear PTOs is demonstrated and could be used in the future for the dimensioning of the PTO elements.
Future development of the model are currently implemented, with the extension of the non-linear model to the 3D case. This will extend again the possibility of the model, but probably at the expense of the computing requirement. It is possible that a mix of 2D and 3D model might be the right level of modelling in the future, depending on the simulation objectives.

VIII. Acknowledgements

This project has been supported by Scottish Enterprise under the framework of the OCEANERA-NET First Joint Call 2014.

IX. Contributions

Rémy Pascal drafted most of the manuscript and established the mooring models (linear and non-linear) with Adrien Combourieu. Benjamin Gendron contributed to the non-linear model, implemented it into InWave and produced the non-linear results.

References

[1] B. Drew, A. R. Plummer, and M. N. Sahinkaya, "A review of wave energy converter technology," *Proceedings of the Institution of Mechanical Engineers, Part A: Journal of Power and Energy*, vol. 223, no. 8, pp. 887–902, dec 2009.

[2] R. C. R. Pascal, A. Torres Molina, and A. Gonzalez Andreu, "Going further than the scatter diagram : tools for analysing the wave resource and classifying sites," in *Proceedings of the 11th European Wave and Tidal Energy Conference*, Nantes, France, 2015, pp. 5–12.

[3] A. Price, "New Perspectives on Wave Energy Converter Control," PhD, The University of Edinburgh, 2009.

[4] F. Sharkey, E. Bannon, M. Conlon, and K. Gaughan, "Dynamic electrical ratings and the economics of capacity factor for wave energy converter arrays," in *Proceedings of the 9th European Wave and Tidal Energy Conference*, Southampton, UK, 2011.

[5] R. C. R. Pascal, Adrien Combourieu, S. Nauwelaerts, and A. Foschini, "Experimental assessment of an innovative concept for managing mooring load," in *Proceedings of 13th European Wave and Tidal Energy Conference*, Cork, Ireland, 2017.

[6] S. H. Salter, J. Cruz, J. Lucas, and R. C. R. Pascal, "Wave powered desalination," in *Proceedings of the International Conference on Integrated Sustainable Energy Resources in Arid Regions*, Abu Dhabi, 2007.

[7] J. Lucas, "The dynamics of a horizontal cylinder oscillating as a wave energy converter about an off-centred axis," PhD, The University of Edinburgh, 2011.

[8] A. Combourieu, M. Philippe, F. Rongère, and A. Babarit, "InWave : A New Flexible Design Tool Dedicated to Wave Energy Converters," *Volume 9B: Ocean Renewable Energy*, 2014.

[9] A. Combourieu, M. Philippe, A. Larivain, and J. Espedal, "Experimental Validation of InWave , a Numerical Design Tool for WECs," in *11th European Wave and Tidal Energy Conference*, 2015, pp. 1–8.

[10] F. Wendt, Y.-h. Yu, K. Nielsen, K. Ruehl, and J. Bunnik, Tim and Touzon, Imanol and Nam, Bo Woo and Kim, Jeong Seok and Kim, Kyong-hwan and Janson, Carl Erik and Jakobsen, Ken-robert and Crowley, Sarah and Vega, Luis and Rajagopalan,, "International Energy Agency Ocean Energy Systems Task 10 Wave Energy Converter Modeling Verification and Validation," in *Proceedings of 13th European Wave and Tidal Energy Conference*, Cork, Ireland, 2017.

[11] R. C. R. Pascal and G. S. Payne, "Impact of motion limits on sloped wave energy converter optimization," *Proceedings of the Royal Society A*, vol. 472, no. 2187, 2016.

[12] R. C. R. Pascal and T. Opalka, "D2.6 Tank Test Report INNOSEA v1 20160824," INNOSEA, Edinburgh, UK, Tech. Rep., 2016.